

Multilayer Al₂O₃/SiC ceramics with improved mechanical behavior

Jihong She*, Takahiro Inoue, Kazuo Ueno

Department of Energy Conversion, Osaka National Research Institute, Midorigaoka 1-8-31, Ikeda, Osaka 563-8577, Japan

Received 5 August 1999; received in revised form 2 February 2000; accepted 5 February 2000

Abstract

Multilayer Al₂O₃/SiC ceramics with a perfect laminated structure were fabricated by extrusion-molding and hot-pressing. The mechanical properties and fracture behavior were evaluated under bending tests. Crack deflection was consistently observed at the interfaces between the Al₂O₃ layers and the SiC-containing interphase. This led to a graceful failure in combination with a high apparent toughness and an increased fracture energy. © 2000 Elsevier Science Ltd. All rights reserved.

Keywords: Al₂O₃; Composites; Hot pressing; Interfaces; Laminates; Mechanical properties; Multilayers; SiC

1. Introduction

The major problem with a widespread application of ceramics as structural components is the lack of reliability in mechanical properties. One way to overcome this problem is to introduce weak interfaces, which deflect a growing crack and thus increase the resistance to fracture. As is well-known, such interfaces can be easily introduced by incorporating fibers into ceramic matrices. However, the fabrication of fiber-reinforced ceramics is time-consuming, complex and expensive. Therefore, some simple and inexpensive processes are expected. Clegg and co-workers^{1,2} developed a cheap and effective process to produce multilayer SiC ceramics with weak graphite interlayers, which had a similar fracture behavior to fiber-reinforced ceramics. Lately, this method was successfully applied to fabricate laminated Si₃N₄/BN ceramics, which exhibited a graceful failure with high toughness and fracture energy due to the presence of weak BN interphase between Si₃N₄ layers.^{3,4} Furthermore, several models^{5–8} were proposed to predict the fracture behavior of layered ceramics in bending.

Recently, a non-catastrophic fracture behavior has been attained in our laboratory for multilayer Al₂O₃-based ceramics with a SiC-containing interphase. Unfortunately, some delamination cracks were observed to kink out of the interface due to the irregularity of the

interphase. This may greatly decrease the energy dissipation capability of layered ceramics during fracture. In the present work, a simple spray technique is used to give a uniform SiC-interphase. The mechanical properties of such a composite are measured on strength, toughness and fracture energy. Moreover, the fracture behavior is investigated, and the crack path is observed.

2. Experimental procedure

Commercially available α -Al₂O₃ (TM-D, Taimei Chemicals Co., Ltd., Japan) and β -SiC (UF grade, Ibi-den Co., Tokyo, Japan) powders, which have an average particle size of 0.22 and 0.27 μ m, were used in this work. To develop a fine-grained microstructure in the Al₂O₃ layers, a high-purity ZrO₂ powder with a mean particle diameter of 0.30 μ m (TZ-8Y, Toyo Soda Manufacturing Co., Ltd., Japan) was added and the volume ratio of Al₂O₃ to ZrO₂ was taken as 82.5:17.5. Green sheets were formed by extrusion and the sheet thickness was fixed at \sim 200 μ m. Subsequently, the sheets were cut into square units of 40 \times 40 mm. To introduce weak interfaces between the Al₂O₃ layers, the surface of each sheet was coated with a 50 vol% SiC-containing slurry by means of a simple spray technique rather than the conventional dip-coating method. This may greatly improve the uniformity of the SiC interphase. After coating, the sheets were dried, stacked and warm-compressed in a graphite die at a temperature of 250°C using a 25-MPa pressure. This temperature–pressure

* Corresponding author. Tel.: +81-727-51-954.

E-mail address: jhshe@hotmail.com (J. She).

condition is sufficient to entirely collapse all the voids between the green sheets. Hot-pressing was performed in vacuum under 20 MPa at 150°C for 1 h and a low heating rate of 5°C/min was used below 600°C to remove the polymers. After hot-pressing, the specimens were cut and ground into rectangular bars with the prospective tensile surface parallel to the layer plane.

Density was measured by the immersion technique in water. Three-point bending strength was determined on three test bars of 3 mm thick, 4 mm wide and 40 mm long at a cross-head speed of 0.5 mm/min. The tensile surfaces were polished and the edges were chamfered. Fracture toughness was measured on four test bars of 4 mm high, 3 mm wide and 40 mm long by a four-point SENB (single edge notched beam) method with a 10-mm inner span and a 30-mm outer span at a cross-head speed of 0.1 mm/min. A straight notch was introduced at the center part of the test bar using a 100- μ m-wide diamond blade and the notch depth was about 1.5 mm. Strength and toughness measurements were performed under displacement control with the tensile surface perpendicular to the direction of the applied load. Data were collected using a computerized data-acquisition system. Fracture energy was calculated from the area under the load-displacement curve of notched bars. Layered structure and crack propagation were observed by optical microscopy.

3. Results and discussion

Fig. 1 presents the cross-sectional micrograph of a representative multilayer specimen. As can be seen, the Al_2O_3 layers (gray regions) and the SiC-containing interphase (dark regions) are reasonably uniform and the interfaces are straight and well-distinguishable. No cracks or delaminations can be detected at the interfaces. The average thickness was determined to be about 90 μ m for the Al_2O_3 layers and 10 μ m for the SiC-containing

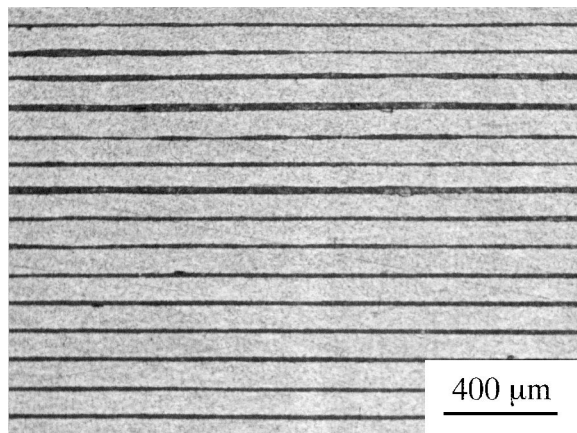


Fig. 1. Optical micrograph of a polished cross-section, showing the multilayered structure of a representative specimen.

interphase. On the other hand, a few of pores were observed in the SiC-containing interphase. By assuming that the Al_2O_3 layers were completely densified, the porosity in the SiC-containing interphase was estimated to be about 42% from the bulk density of the layered specimen and the volume fraction of the SiC interphase.

Fig. 2 shows a typical load-displacement curve of un-notched specimen during a three-point bending test. As shown, the load remains linear up to the peak load, at which point a crack initiates from some surface defects and grows quickly in the through-thickness direction, giving rise to the first load drop. However, such a crack did not travel across the specimen, but was arrested and deflected by the adjacent SiC-containing interphase. As indicated in Fig. 3, the transverse crack deflects at the interface between the Al_2O_3 layer and the SiC interphase. Such interfacial delamination allows the measured load to continue rising, until some new cracks form in the second Al_2O_3 layer. This process is repeated

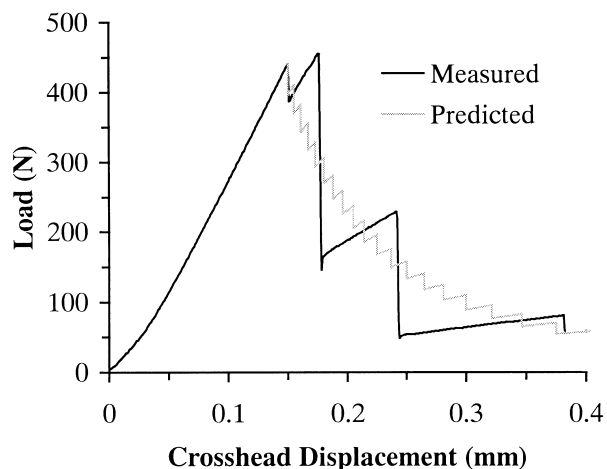


Fig. 2. Load-displacement curve of an un-notched specimen under a three-point bending test.

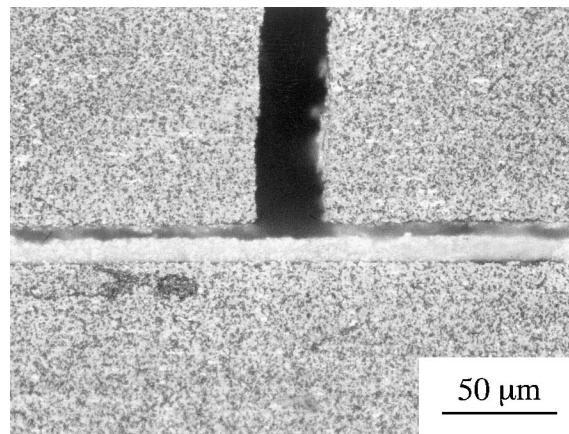


Fig. 3. High-magnification optical micrograph showing the deflection of a through-thickness crack by the interphase.

as the Al₂O₃ layers crack, resulting in a sawtooth load–displacement response. The tip and root of the saw teeth correspond to the points at which the crack initiates and arrests, respectively. From the theoretical analysis⁷ and experimental work⁸ on the flexural stress–strain response of brittle multilayer materials, the nominal stresses, σ_i and σ_i^* , at the tip and root of the *i*th saw tooth in the load–displacement curve can be given by

$$\sigma_i = \sigma_o \left(1 - \frac{N_i}{N_o}\right)^2$$

and

$$\sigma_i^* = \sigma_o \left(1 - \frac{1}{N_o - N_i}\right)^3 \left(1 - \frac{N_i}{N_o}\right)^2$$

where N_o is the total number of layers, N_i is the number of cracked layers, and σ_o is the initial matrix cracking stress, which can be calculated from⁸

$$\sigma_o = \frac{3P_o L}{2B(N_o t)^2}$$

where P_o is the applied load leading to the initial matrix cracking, L is the supporting span of the three-point bending fixture, B is the specimen width and t is the thickness of the individual layers. It can be seen in Fig. 2 that the load–displacement responses are essentially similar between the theoretical prediction and experimental measurement. In the theoretical analysis, the strengths of the individual layers are assumed to be equivalent. Consequently, the layers crack sequentially in order of their positions and the loads follow a step-like reduction beyond the initial cracking event. In the testing process, however, cracking was found to occur disorderly with respect to their positions. This is thought to be due to the relatively broad distribution in the strengths of the layers. In some instances, several layers were observed to crack simultaneously, resulting in a relatively large interval of displacement, as shown in Fig. 2. By assuming that each of the cracking events cause 6 layers to crack at the same time, the predicted and measured load–displacement responses are compared in Fig. 4. Clearly, the predicted curve is in good agreement with the experimental measurement.

Fig. 5 is an optical micrograph of the side surface of an un-notched specimen after flexural testing. It is clear in this micrograph that the through-thickness cracks are extensively deflected between all the Al₂O₃ layers. This may lead to a high energy dissipation during crack growth. In the present work, the average fracture energy was measured to be 3335 J/m². On the other hand, it can be seen in Fig. 6 that the sites of the through-thickness cracks are distributed in a more or less random fashion. This suggests that the stress concentrations associated

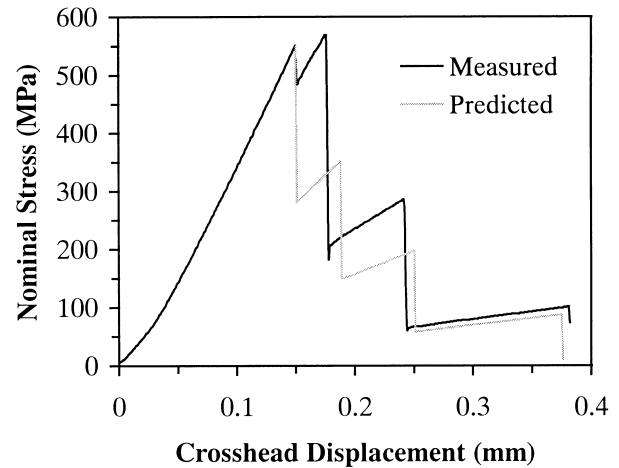


Fig. 4. Comparison of the measured and predicted stress–displacement curves for a 30-layer specimen.

with the transverse cracks are small and thus have little influence on the cracking sites in the adjacent Al₂O₃ layers. In fact, such cracks initiate from some processing flaws within the Al₂O₃ layers. If these flaws are eliminated, a large increase in fracture energy should be expected.

Fig. 6 shows a representative curve of applied load versus crosshead displacement for a notched specimen. Evidently, the sequence of events leading to failure in the notched specimen is similar to that described above for the un-notched specimen, although the transverse crack initiates from the notch tip in the notched specimen but from some surface flaws in the un-notched specimen. From the maximum load in the load–displacement curve, the fracture toughness was calculated using the following equation⁹

$$K_{IC} = \frac{3}{2} \cdot \frac{P(S_o - S_i)}{BW^{3/2}} \cdot \frac{\alpha^{1/2}}{(1 - \alpha)^{3/2}} \cdot Y$$

where P is the applied peak load, S_i and S_o are the inner and outer loading span, B is the specimen width, W is the specimen thickness, α is the ratio of notch depth to specimen thickness (a/W), and Y is a geometrical factor:

$$Y = 1.9887 - 1.326\alpha - \frac{(3.49 - 0.68\alpha + 1.35\alpha^2)\alpha(1 - \alpha)}{(1 + \alpha^2)}$$

In this work, the average “toughness” was calculated to be 15.1 MPam^{1/2}. For some specimens, the apparent toughness up to 18.5 MPam^{1/2} and the fracture energy in excess of 4900 J/m² were achieved.

To determine the effects of loading rate on toughness and fracture energy, a low crosshead speed of 0.05 mm/min was applied. As can be seen in Table 1, the average toughness decreased to 10.9 MPam^{1/2} at a crosshead speed of 0.05 mm/min, but the fracture energy did not show the sensitivity to the loading rate.

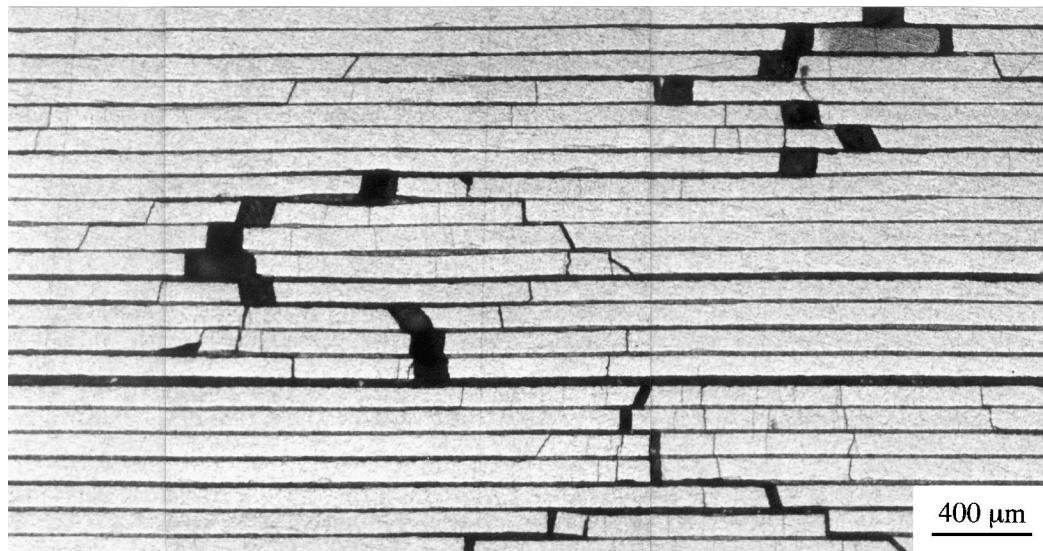


Fig. 5. Overall view of the side surface of an un-notched specimen after testing.

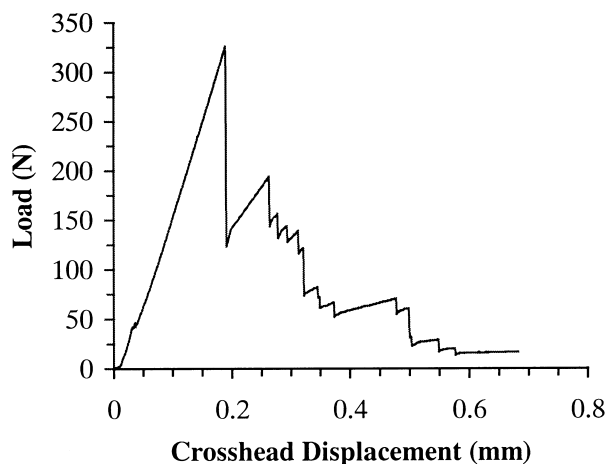


Fig. 6. Applied load as a function of crosshead displacement for a notched specimen.

Table 1
Effect of loading rate on the mechanical properties of multilayer $\text{Al}_2\text{O}_3/\text{SiC}$ ceramics

Property	Crosshead speed (mm/min)		
	0.5	0.1	0.05
Bending strength (MPa)	563 ± 41	–	–
Apparent toughness ($\text{MPam}^{1/2}$)	–	15.1 ± 2.0	10.9 ± 2.9
Fracture energy (J/m^2)	–	335 ± 872	3385 ± 476

4. Conclusions

Multilayered Al_2O_3 ceramics with a weak SiC-containing interphase were fabricated by extrusion-molding and hot-pressing. The mechanical properties and fracture behavior were examined in bending. Due to the deflection

of cracks along the weak interfaces, a non-catastrophic fracture was observed. The bending strength, apparent toughness and fracture energy were, respectively, up to 563 MPa, $15.1 \text{ MPam}^{1/2}$ and 3335 J/m^2 . Moreover, improved damage tolerance and fracture resistance behavior are expected. A further investigation on this topic is currently under way.

Acknowledgements

J.S. wishes to acknowledge the Agency of Industrial Science and Technology (AIST), Ministry of International Trade and Industry (MITI) for granting him an AIST Research Fellowship at Osaka National Research Institute, Japan.

References

1. Clegg, W. J., Kendall, K., Alford, N. M., Button, T. W. and Birchall, J. D., A simple way to make tough ceramics. *Nature*, 1990, **347**, 455–457.
2. Clegg, W. J., The fabrication and failure of laminar ceramic composites. *Acta Metall. Mater.*, 1992, **40**, 3085–3093.
3. Liu, H. and Hsu, S. M., Fracture behavior of multilayer silicon nitride/boron nitride ceramics. *J. Am. Ceram. Soc.*, 1996, **79**, 2452–2457.
4. Kovar, D., Thouless, M. D. and Halloran, J. W., Crack deflection and propagation in layered silicon nitride/boron nitride ceramics. *J. Am. Ceram. Soc.*, 1998, **81**, 1004–1012.
5. Phillipps, A. J., Clegg, W. J. and Clyne, T. W., Fracture behavior of ceramic laminates in bending: I. Modelling of crack propagation. *Acta Metall. Mater.*, 1993, **41**, 805–817.
6. Phillipps, A. J., Clegg, W. J. and Clyne, T. W., Fracture behavior of ceramic laminates in bending: II. Comparison of model

- predictions with experimental data. *Acta Metall. Mater.*, 1993, **41**, 819–827.
7. Folsom, C. A., Zok, F. W. and Lange, F. F., Flexural properties of brittle multilayer materials: I. Modeling. *J. Am. Ceram. Soc.*, 1994, **77**, 689–696.
 8. Folsom, C. A., Zok, F. W. and Lange, F. F., Flexural properties of brittle multilayer materials: II. Experiments. *J. Am. Ceram. Soc.*, 1994, **77**, 2081–2087.
 9. Munz, D., Bubsey, R. T. and Shannon, J. L., Fracture toughness determination of Al_2O_3 using four-point-bend specimens with straight-through and chevron notches. *J. Am. Ceram. Soc.*, 1980, **63**, 300–305.